Zoosyst. Evol. 101 (2) 2025, 761–778 | DOI 10.3897/zse.101.142007

PENSOFT.

MUSEUM FÜR NATURKUNDE BERLIN

Two new species of *Idas* (Bivalvia, Mytilidae) from sunken wood in the East China Sea: description, phylogenetic position and symbionts

Qiong Wu[1,2], Yi-Tao Lin[3], Jian-Wen Qiu[3], Mei Yu Xu[4], Bing Peng Xing[1]

1 *Third Institute of Oceanography Ministry of Natural Resources, Xiamen, Fujian, China*
2 *College of Life Sciences, Beijing Normal University, Beijing, China*
3 *Department of Biology, Hong Kong Baptist University, Hong Kong, China*
4 *Unaffiliated, Guangzhou, China*

https://zoobank.org/CA51086B-C1D5-4908-B745-612F26276076

Corresponding author: Bing Peng Xing (xingbpeng@gmail.com)

Academic editor: M. Glaubrecht ♦ **Received** 17 November 2024 ♦ **Accepted** 26 March 2025 ♦ **Published** 10 April 2025

Abstract

Mussels of the genus *Idas* (Bathymodiolinae) are small bivalves inhabiting organic falls and cold seep ecosystems. Despite their ecological significance, the taxonomy and phylogeny of *Idas* remain understudied. In this study, 30 *Idas* specimens were collected from a piece of sunken wood in the East China Sea at depths of 460–550 m. DNA barcoding and phylogenetic analysis revealed three distinct clades: 23 specimens matched *Idas* sp. ESU D, previously reported from Japan and the Philippines, five samples clustered with *Idas iwaotakii* (Habe, 1958), and two samples formed a new clade related to *I. iwaotakii*. These findings resulted in the description of two new species, *Idas sinensis* **sp. nov.** and *Idas pacificus* **sp. nov.** We present the complete mitochondrial genomes for both species and investigate the diversity of their symbiotic microbes through full-length 16S rRNA amplicon sequencing. Phylogenetic analyses of mitochondrial genomes further support the taxonomic placement of the new species. The gill-associated microbial communities of these mussels include sulfur-oxidizing SUP05 bacteria, suggesting chemosynthetic symbiosis.

Key Words

Bathymodioline, Chemosynthesis, *Idas*, Mitochondrial genome, Sunken wood

Introduction

Mussels are among the most common organisms found in hydrothermal vent and cold seep ecosystems (Kiel 2010; Xu et al. 2019). However, the origins of deep-sea chemosynthetic symbiotic species remain a subject of debate due to the scarcity of chemosynthetic fossil evidence (Genio et al. 2012). Earlier researchers suggested that these species represent ancient lineages that survived extinction events (Newman 1985; McArthur and Tunnicliffe 1998). In contrast, recent evidence increasingly supports the hypothesis that mollusks in chemosynthetic ecosystems may have originated through adaptive radiation from shallow marine environments. In this context, sunken wood likely served as "stepping stones" facilitating the transition from shallow to deep-sea habitats (Distel et al. 2000; Romano et al. 2020; Altamia et al. 2024). This hypothesis is logically plausible. Geographically, sunken wood, originating from terrestrial sources, is commonly found along continental margins (Pailleret et al. 2007), potentially providing a substrate for mollusks to transition from shallow-water to deep-sea environments (Altamia et al. 2024). Energetically, wood provides an essential food source in the nutrient-scarce deep sea (Pop Ristova et al. 2017). Due to the difficulty of metabolising lignin and cellulose, sunken wood communities generally rely on organisms equipped with specific enzymes that convert these materials into bioavailable forms, with microbes playing an essential role in this process (Turner 1973; Bienhold et al. 2013). As symbiotic dependence increases and digestive tracts degrade, colonization of these environments naturally follows

Copyright *Wu, Q. et al.* This is an open access article distributed under the terms of the Creative Commons Attribution License (CC BY 4.0), which permits unrestricted use, distribution, and reproduction in any medium, provided the original author and source are credited.

(Lorion and Samadi 2010). From a redox perspective, the decomposition of plant and animal remains releases hydrogen sulfide, generating reducing conditions similar to those at hydrothermal vents. Such environments provide favorable conditions for benthic organisms to transition into chemosynthetic symbiosis (Distel et al. 2000; Bernardino et al. 2010). Molecular evidence further supports this hypothesis: Samadi et al. (2007) demonstrated that all mytilids associated with seeps, vents, sunken wood, and large animal carcasses form a monophyletic group, with species inhabiting organic falls occupying the basal positions on the phylogenetic tree. However, this hypothesis has been challenged by some opposing evidence. For instance, in the phylogenetic trees constructed by McCowin et al. (2020) and Lorion et al. (2013), *Vulcanidas insolatus* Cosel & B. A. Marshall, 2010,, a vent mussel, appears in a more basal branch than the lineage of wood-fall species. In recent years, with the increasing research into hydrothermal vents and cold seeps, molecular data for bathymodioline mussels from these habitats in waters surrounding China have been increasingly published (Lin et al. 2022; Wang et al. 2022; Li et al. 2023). However, compared to species from vents and seeps, our understanding of species associated with organic falls remains limited (Lorion et al. 2010; Lorion and Samadi 2010).

The genus *Idas* (Bathymodiolinae) was established based on samples collected from the North Atlantic (Jeffreys 1876). Members of *Idas* are small mussels widely distributed in organic fall and cold seep habitats (Lorion et al. 2012). Small bathymodioline mussels, such as those in the genus *Idas*, provide insights into a potential evolutionary pathway from organic falls to vents and seeps (Duperron et al. 2008a). Species of *Idas* are known for their extracellular symbionts and the flexibility of their symbiotic relationships, with some species harboring up to six chemosymbiotic bacteria (Duperron et al. 2008a), with others having lost their symbionts (Rodrigues et al. 2015). However, the diversity of this genus remains poorly understood, with only 14 named species currently recognized (WoRMS 2024). Some specimens considered to be *Idas* have not been formally described (Duperron et al. 2008b; Lorion et al. 2009; Lorion et al. 2012; Rodrigues et al. 2015). Due to morphological convergent evolution and the lack of molecular data, the classification of many bathymodioline species associated with organic falls remains unresolved. Some genera have been confirmed as polyphyletic (Thubaut et al. 2013b; McCowin et al. 2020), and the relationship between *Idas* and *Adipicola* remains unclear (Mietto et al. 2019). This classification mainly follows the works of Altamia et al. (2024), Lin et al. (2022), and Xu et al. (2019). However, some of the genus names employed in these studies, such as "Lignomodiolus" (Thubaut et al. 2013b) and "*Nipponiomodiolus*" (Samadi et al. 2015), remain unresolved and are considered nomena nuda.

The Pacific region is considered to be the origin of deep-sea mussels (Kyuno et al. 2009). Investigating wood-fall mussels in this area can provide crucial insights into the early evolutionary history of deep-sea mussels (Lorion and Samadi 2010). In 2023, we collected a piece of sunken wood from the East China Sea and obtained 30 specimens of *Idas* from it. DNA barcoding revealed that these samples formed three major clades: 23 of these specimens are closely related to *Idas* sp. ESU D, which was collected from Japanese and Philippine waters at depths of 760 to 1760 meters (Lorion et al. 2013). Five samples clustered with *Idas iwaotakii*, while two samples formed a distinct clade, constituting a sister group to *I. iwaotakii*. Apart from *I. iwaotakii*, the morphology of the remaining two species can be distinguished from all known *Idas* species in the Western Pacific region. In this study, we describe these two species based on an integrative analysis of their morphology and molecular phylogenetic position. Additionally, we present the complete mitochondrial genomes of the *Idas* genus for the first time and determine the diversity of their symbionts using full-length bacterial 16S amplicon sequencing. These findings provide valuable data for the biodiversity of wood-fall ecosystems and the gene flow of symbionts in the East China Sea and surrounding regions.

Materials and methods

Sample collection and photography

In April 2023, a piece of sunken wood, approximately 35 cm in length, was collected by a trawler in the East China Sea (30.7°N, 127.8°E) at approximately 460–550 m depth (Suppl. material 1). The wood sample was stored at -30 °C on board. After being transferred to the laboratory, the wood sample was cut open using a saw to collect the specimens inside. The specimens were preserved in 95% ethanol and stored at -80 °C. All type specimens involved in this study are housed in the specimen collection at the Third Institute of Oceanography, Ministry of Natural Resources (TIO).

Photographs were taken using a Leica S9D stereomicroscope and an MC170-HD digital camera.

DNA extraction, PCR amplification, and sequencing

The mantle, adductor muscle, and foot were dissected and used for extraction of the host DNA, while the gill was used to extract bacterial DNA. For some samples that were poorly preserved or too small, the entire soft tissue was used for DNA extraction. Total DNA from all body parts was extracted using the Qiagen DNeasy Blood & Tissue Kit following the manufacturer's instructions, and the DNA quality was assessed using NanoDrop.

The mitochondrial c oxidase subunit I (cox1) and 16S ribosomal RNA (16S) were obtained according to the method described by Meyer (2003), Olu-Le Roy et al. (2007) and Baco-Taylor (2002). The PCR reactions were conducted in 25 μL solution, containing 12.5 μL PCR mixture (Taq plus Master Mix II (Dye Plus)), 1 μL of each

Table 1. PCR primers, reaction conditions, and references.

Gene	Primer F	Primer R	Reaction Condition	Reference
cox1	dgLCO1490: 5′-GGTCAACAAATCATAAAGAYATYGG-3′	dgHCO2198: 5′-TAAACTTCAGGGTGA CCAAARAAYCA-3′	95 °C/3min; 95 °C/55s, 45 °C/1min(+0.5 °C/cycle), 72 °C/1min, 15cycle; 95 °C/50s, 49 °C/1min, 72 °C/1min, 20 cycle; 72 °C/10min	Meyer (2003)
cox1	BathCOI-F: 5′-TGTGGTCTGGAATAATTGGAAC-3′	BathCOI-R: 5′-ATAAAAAGATGTATTRAARTGACG-3′	95 °C/3min; 95 °C/35s, 48 °C/35s, 72 °C/70s, 5 cycle; 94 °C/35s, 52 °C/35s, 72 °C/70s, 35cycle; 72 °C/10min	Olu-Le Roy, Von Cosel et al. (2007)
16s rRNA	LRJ-12864: 5′-CTCCGGTTTGAACTCAGATCA-3′	Idas 16SA: 5′-GGARGTASGCCCTGCCCWATGC-3′	95 °C/5min; 95 °C/40s, 55 °C/50s, 72 °C/60s, 34 cycle; 72 °C/10mins	Baco-Taylor (2002)

primer, 2.5 µL template, and 8 µL ultrapure water. Reaction conditions are shown in Table 1. All PCR products were evaluated for amplification efficiency using 1% agarose gel electrophoresis and sequenced at Sangon Biotech (Shanghai) Co., Ltd.. The sequences were aligned and trimmed the ends with low signal strength using SeqMan v. 7.1.0 (DNAStar, U.S.A.).

Phylogenetic analysis

The bathymodioline sequences obtained in this study and sequences of representative species were also obtained from GenBank for phylogenetic analysis. The list of sequences corresponding to those in Lin et al. (2022) (Suppl. material 4). Multiple sequences will be aligned with MAFFT (Katoh and Standley 2013) using the 'auto' strategy and codon (cox1) /normal (16S) alignment mode. The cox1 sequences were further refined using MACSE (Ranwez et al. 2018). Ambiguously aligned fragments were removed using Gblocks (Talavera and Castresana 2007). PhyloSuite (Zhang et al. 2020) was used to concatenate the sequences from different genes. Operational taxonomic units (OTUs) were delimited using the Automatic Barcode Gap Discovery (ABGD) method (Puillandre et al. 2012) via the online tool (https://bioinfo.mnhn.fr/abi/public/abgd/abgdweb.html), based on the COX1 sequence.

The best-fit partition model for both IQ-TREE (Guindon et al. 2010; Nguyen et al. 2015) and MrBayes (Ronquist et al. 2012) was selected using ModelFinder (Kalyaanamoorthy et al. 2017) based on the AIC criterion. For coding sequence (CDS) genes, the codon model was applied, selecting the optimal model for each codon position individually. Bayesian inference phylogenies were inferred using MrBayes (v3.2.6) (Ronquist et al. 2012) under the partition model (2 parallel runs, 2,000,000 generations), with the initial 25% of sampled data discarded as burn-in. Maximum likelihood (ML) phylogenies were inferred using IQ-TREE (Nguyen et al. 2015) under the edge-linked partition model with 5000 ultrafast bootstrap replicates and approximate Bayes test (Anisimova et al. 2011), and the Shimodaira–Hasegawa–like approximate likelihood-ratio test (Guindon et al. 2010). The phylogenetic trees were viewed and edited using iTOL (https://itol.embl.de/) (Letunic and Bork 2021).

Mitochondrial genome sequencing

Total genomic DNA was extracted from three individuals of *I. pacificus* sp. nov. and one individual of *Idas sinensis* sp. nov. using the Qiagen DNeasy Blood & Tissue Kit, following the manufacturer's instructions. The samples were submitted to Shanghai Majorbio Bio-pharm Technology Co., Ltd for library preparation and Illumina sequencing. The DNA was fragmented into random pieces using ultrasound, followed by end-repair, 3′-adenine addition, and adapter ligation. The DNA fragments were then enriched for approximately 400 bp genomic segments using magnetic beads and PCR amplification to generate the sequencing library. The DNA libraries were sequenced on the Novaseq 6000 platform to produce 150 bp paired-end reads. The quality of the sequencing raw data was evaluated using FastQC (Andrews 2010). The sequences were assembled and preliminarily annotated using MitoZ (Meng et al. 2019). Sequencing depth was assessed using Burrows-Wheeler Aligner (BWA) (Li 2013) and Samtools (Danecek et al. 2021).

Protein-coding gene (PCG) boundaries were adjusted by aligning sequences with related species using Nucleotide BLAST (BLASTn) and Protein BLAST (BLASTp) (*Gigantidas vrijenhoeki* S.-J. Jang, P.-T. Ho, S.-Y. Jun, D. Kim & Y.-J. Won, 2020; genbank accession number: NC_068739), and the positions of the start and stop codons were confirmed using SnapGene (v7.1.2). rRNA annotation was performed using MitoZ, with the process completed by calling infernal-1.1.1 (Nawrocki and Eddy 2013; Meng et al. 2019). tRNA annotations were corrected using tRNAscan-SE (Chan et al. 2021). Atp8 was manually annotated between nad3 and s-rRNA using Find Open Reading Frames (ORFs) (Lee et al. 2019). GC skew (= (G–C)/(G+C)) and GC content were calculated and mitochondrial circular plots were generated using proksee (https://proksee.ca/) (Grant et al. 2023). Mitochondrial gene arrangement patterns were determined using PhyloSuite (Zhang et al. 2020) and visualized with iTOL (Letunic and Bork 2021).

Mitochondrial genome-based phylogenetic tree

Mitochondrial genomes of 24 species from GenBank and 2 species (4 individuals) obtained in this study were used for phylogenetic analysis. Three *Mytilus* species were

used as outgroups (Liu et al. 2018; Lee et al. 2019). The concatenated sequences from 12 PCGs and two RNA (rRNA) genes were used to construct the phylogenetic tree. Due to the high variability in tRNA numbers (Lee et al. 2019) and the high variability in atp8 sequences (Zhao et al. 2022), these genes were excluded from the analysis.

The best partitioning scheme and evolutionary models for partitions were selected using PartitionFinder2 (Lanfear et al. 2017) with a greedy algorithm and AIC criterion. All other procedures were the same as for the phylogenetic analysis for the cox1 + 16S data.

16S rRNA amplicon sequencing and data analysis

Since the wood sample was collected by a commercial benthic trawler and stored at -30 °C in a freezer without immediate fixation, it was not possible to perform fluorescence in situ hybridization. The potential symbionts were inferred using full-length 16S rRNA amplicon sequencing. Only a subset of samples with successfully dissected gill tissues were used for this analysis.

PCR reactions and sequencing were performed as a commercial service at Shanghai Majorbio Bio-pharm Technology Co., Ltd. The primers used were 27F(AGRGTTYGATYMTGGCTCAG) and 1492R(RGYTACCTTGTTACGACTT) (Weisburg et al. 1991). Primers were tailed with PacBio barcode sequences to distinguish each sample. The PCR was conducted using an ABI GeneAmp 9700, with Kapa Biosystems KAPA HiFi DNA Polymerase. The reaction mixture consisted of 10 µl 2×Pro Taq, 0.8 µl Forward Primer (5 µM), 0.8 µl Reverse Primer (5 µM), 10 ng/µl Template DNA, and ddH_2O to a total volume of 20 µl. The PCR program included an initial denaturation at 95 °C for 3 minutes, followed by 29 cycles of 95 °C for 30 seconds, 60 °C for 30 seconds, 72 °C for 45 seconds, and a final extension at 72 °C for 10 minutes. PCR products were purified using the AMPure® PB beads (Pacifc Biosciences, CA, USA) and quantified with Qubit 4.0 (Thermo Fisher Scientific, USA).

Purified products were pooled in equimolar and DNA library was constructed using the SMRTbell prep kit 3.0 (Pacifc Biosciences, CA, USA) according to PacBio's instructions. Purified SMRTbell libraries were sequenced on the Pacbio Sequel IIe System (Pacifc Biosciences, CA, USA). High-fidelity (HiFi) reads were obtained from the subreads, generated using circular consensus sequencing via SMRT Link (v11.0). Raw data quality was assessed using fastp (v0.19.6) (Chen et al. 2018). Barcode-CCS recognition was performed using Lima (https://lima.how/). ASV (Amplicon Sequence Variant) information was obtained using DADA2_CCS (Callahan 2022) (https://benjjneb.github.io/dada2/). ASVs aligned to chloroplasts and mitochondria were removed, along with ASVs with a relative abundance below 0.001. Sequences were rarefied to the minimum sample size. Taxonomic annotation was performed using the silva138.1/16s_bacteria database. ASV analyses, including sample filtering and sequence rarefaction, generation of Venn diagrams, community bar plots, and heatmaps, were performed using Majorbio Cloud 2024 (cloud.majorbio.com). ML phylogenetic trees were constructed using PhyloSuite (Zhang et al. 2020) following the same procedures as in the previous section. Microbial functions were predicted using FAPROTAX (Louca et al. 2016).

Results and discussion

Other fauna on the sunken wood

The biological community on the sunken wood is closely related to both the wood species (Pailleret et al. 2007) and the successional stage of the wood-associated community (Bernardino et al. 2010; Bienhold et al. 2013). These factors are crucial for determining the successional stage of the sample and, in turn, inferring the developmental stage of the mussels. However, due to the potential loss of some organisms caused by water flow during trawling (Pailleret et al. 2007), we did not conduct a quantitative assessment of the individual numbers of each species.

The most abundant species on the sunken wood collected in this study was *Pectinodonta aurora* B. A. Marshall, Puillandre, Lambourdière, Couloux & Samadi, 2016, predominantly consisting of mature individuals. The surface of the wood was covered with characteristic feeding pits made by this species (Suppl. material 1). Additionally, members of the families Teredinidae and Xylophagaidae were present, along with their calcareous tubes. Other organisms included small numbers of sea urchins, *Calagrassor* species, and polychaetes, among others. A detailed species list and their respective DNA barcode GenBank accession numbers are provided in Suppl. material 5.

Phylogenetic trees based on cox1 and 16S sequences

The trimmed 16S gene was 404 bp long, and the cox1 sequence was 588 bp long (GenBank accession numbers are listed in Suppl. material 6). The best-fit models according to AIC are provided in Suppl. material 7. The resulting ML and BI phylogenetic trees show some structural differences. Since the ML tree had higher support at the nodes, only the ML tree is presented in the main text, while the BI tree is shown in Suppl. material 2.

Due to some confusion in the systematics of the genera *Idas* and *Adipicola* (Gustafson et al. 1998; Mietto et al. 2019), this study follows Thubaut et al. (2013b), Thubaut et al. (2013a), and Genio et al. (2015) in treating *Adipicola iwaotakii* (Habe, 1958) as *Idas iwaotakii* (Habe, 1958) based on molecular evidence. Therefore, among the recognized species of *Idas*, the following four species have been recorded in the Pacific region: *I. coppingeri* (Murray et al. 1885), *I. indicus* (Smith 1899), *I. washingtonius* (Kyuno et al. 2009; Harbo and Gillespie 2021), and *I. iwaotakii* (Kyuno et al. 2009).

The ABGD analysis revealed that, aside from *Modiolus rumphii* which was used as an outgroup, the remaining sequences could be divided into 51 OTUs. Among these, five OTUs contain more than one sequence that was classified as different species/ESUs in previous studies (Fig. 1: OTU-18, OTU-29, OTU-33, OTU-34 and OTU-45). Both the phylogenetic tree and the ABGD analysis support the clustering of the 30 samples collected in this study into four distinct OTUs (Fig. 1: OTU-47, OTU-48, OTU-49, and OTU-51). Apart from the clade containing *I. iwaotakii*, the other two branches represent the newly described species in this study, temporarily referred to as *Idas* sp. OTU-47 and *I.* sp. OTU-51. Among these, *Idas* sp. OTU-47 forms a sister group with *I. iwaotakii*, while *Idas* sp. OTU-51 is a sister group to *Idas* sp. ESU C. Regarding the clade containing *I. iwaotakii*, sample TIO2023-1816B28 is particularly noteworthy. Although the terminal containing this sample clusters within *I. iwaotakii*, its cox1 sequence shows only 92% similarity to known *I. iwaotakii* sequences. This suggests that the sample may belong to the "species complex within the *Adipicola* (*Idas*) genus" as described by Lorion et al. (2009).

We acknowledge the limitations of using mitochondrial genomes to reconstruct phylogenetic trees. Factors such as incomplete lineage sorting (McGuire et al. 2007; Kimball et al. 2021), introgression, doubly uniparental inheritance (DUI) (Walker et al. 2006; Doucet-Beaupré et al. 2010), maternal inheritance, and recombination can complicate mtDNA interpretations (Rubinoff et al. 2006), making it less suitable as the sole data source for phylogenetic analysis. However, the relatively higher mutation rate of mitochondrial genomes compared to nuclear genomes (Saccone et al. 1999) makes them particularly useful for resolving phylogenetic relationships at lower taxonomic levels. Given the high dispersal potential of organic fall mussel larvae, populations separated by thousands of kilometers may still exhibit close phylogenetic relationships (Fukasawa et al. 2015; DeLeo et al. 2022). Therefore, selecting rapidly evolving genes for phylogenetic tree construction may provide higher resolution in such cases. Furthermore, we compared our phylogenetic tree with that of Lin et al. (2022), which incorporated both mitochondrial and nuclear genes, and found similar topologies, further supporting the reliability of our inferred branching pattern.

General features of the mitochondrial genomes of *Idas pacificus* sp. nov. and *Idas sinensis* sp. nov.

We obtained the mitochondrial genomes of four individuals from the two species, *Idas* sp. OTU-47 and *Idas* sp. OTU-51 (PQ541016–PQ541019, Suppl. material 3). The average sequencing depth of the four samples ranged from 7,915 to 7,940. Among them, the mitochondrial genomes of three *Idas* sp. OTU-51 specimens were assembled into a circular form, with genome sizes ranging from 17,234 bp to 17,480 bp. Each genome includes 23 transfer RNA (tRNA) genes (including 2 trnS and 2 trnL), 13 PCGs, and 2 rRNA genes, with an AT content of 66.67%. The mitochondrial genome of the *Idas* sp. OTU-47 specimen was not circularized, with the assembled portion measuring 17,742 bp. This genome also includes 23 tRNA genes (including 2 trnS and 2 trnL), 13 PCGs, and 2 rRNA genes, with an AT content of 67.91%. The GC skewness values for both species are positive. Except for trnT, all other genes are located on the heavy strand.

Phylogenetic tree and mitochondrial gene arrangement

The topologies of the BI and ML mitochondrial phylogenetic trees are congruent, with the exception of the relationship between *Bathymodiolus marisindicus* and *B. brooksi* (Fig. 2). In our phylogenetic analysis, the genera *Bathymodiolus*, *Idas*, and *Gigantidas* cluster within the subfamily Bathymodiolinae. The clade containing the genus *Modiolus* is sister to Bathymodiolinae, which is consistent with previous analyses (Liu et al. 2018). Both the mitochondrial genome phylogenetic tree and the cox1+16S phylogenetic tree are congruent in topology with those of Xu et al. (2019) in that *Gigantidas japonicus* and *G. securiformis* belong to the genus *Gigantidas* rather than *Bathymodiolus*. Among the species analyzed, the subfamily Bathymodiolinae exhibits shorter branch lengths. Unlike the phylogenetic tree from Lin et al. (2022), the phylogenetic tree based on the 12 PCGs and two rRNA genes reveals a sister relationship between *Bathymodiolus* and *Gigantidas*.

The orders of PCGs and rRNA are relatively conserved within the subfamily Bathymodiolinae and the genus *Modiolus* (Fig. 2), consistent with previous studies (Lee et al. 2019). The arrangement of tRNA genes also exhibits significant conservation within the subfamily Bathymodiolinae. Specifically, the presence of two trnL copies flanking atp8 and one trnS adjacent to rrnL on each side is generally a common characteristic of *Bathymodiolus*, with the exception of *Bathymodiolus brooks*.

Taxonomy

Family Mytilidae Rafinesque, 1815
Genus *Idas* Jeffreys, 1876

***Idas sinensis* sp. nov.**

https://zoobank.org/F28DA47C-082B-40FD-9B47-CECB0BF1D19C

Figs 3H–I, 4F–G

(*Idas* sp. OTU-47 mentioned earlier)

Materials examined. Two specimens collected from the same piece of sunken wood by trawling from a seabed at a depth of 460–550 m (30.7°N, 127.8°E) in April 2023.

Type material. ***Holotype*** • TIO2023-1816B6 (length: 9.3 mm); ***Paratype*** • TIO2023-1816B21 (length: 13.4 mm), with a fractured right valve.

Diagnosis. Shells extremely thin, with internal surface color similar to external surface. Dorsal and ventral margins nearly parallel. Bristles short, brown, mainly concentrated along both sides of ridge in posterior triangular

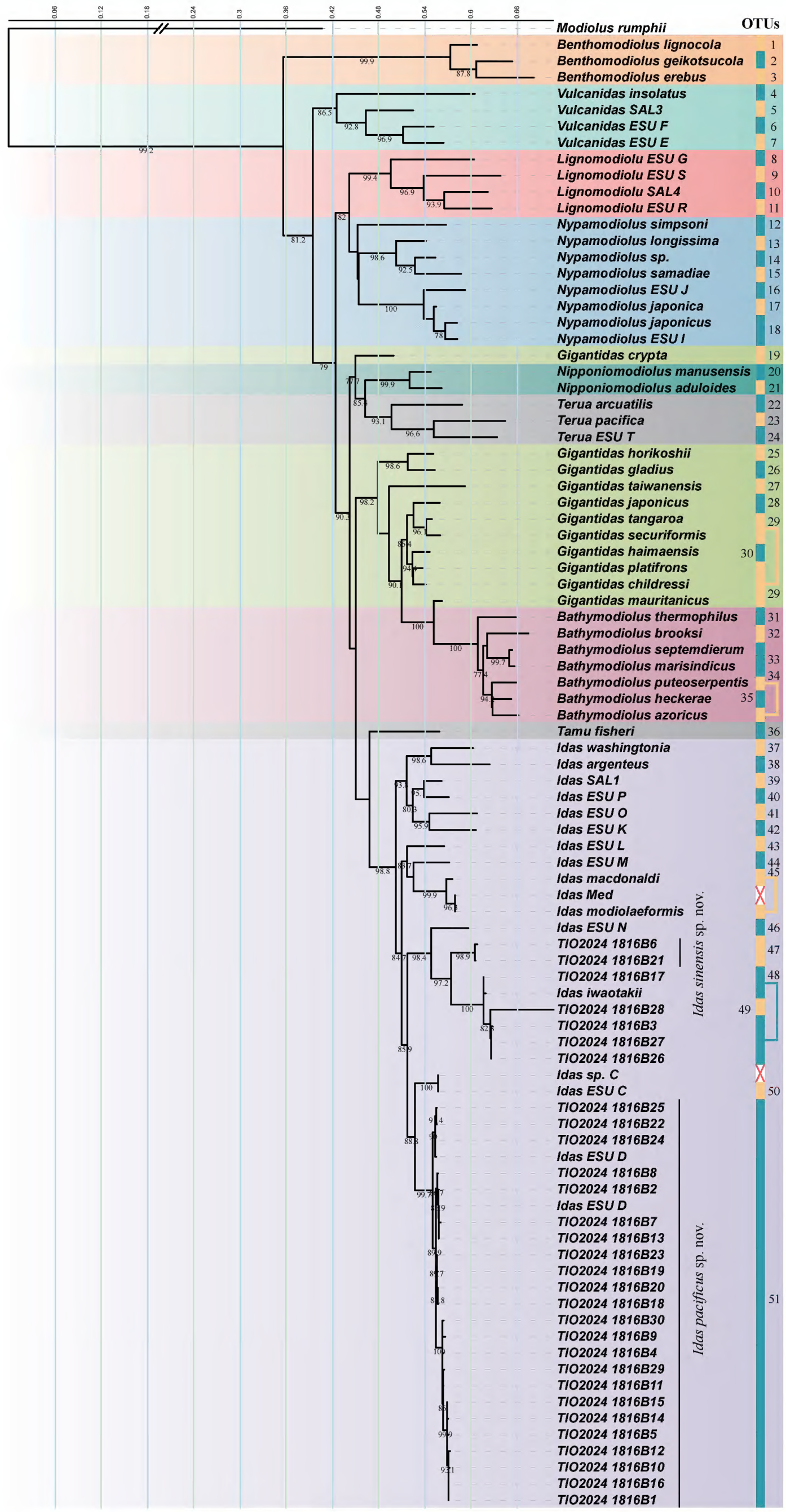

Figure 1. ML phylogenetic tree of the subfamily Bathymodiolinae based on the cox1 and 16S genes. Numbers near the nodes represent bootstrap values (only values >75% are shown). Different genera are distinguished by colors. OTUs are annotated with color blocks and numbers following the species names. Red crosses indicate leaves without cox1 gene data.

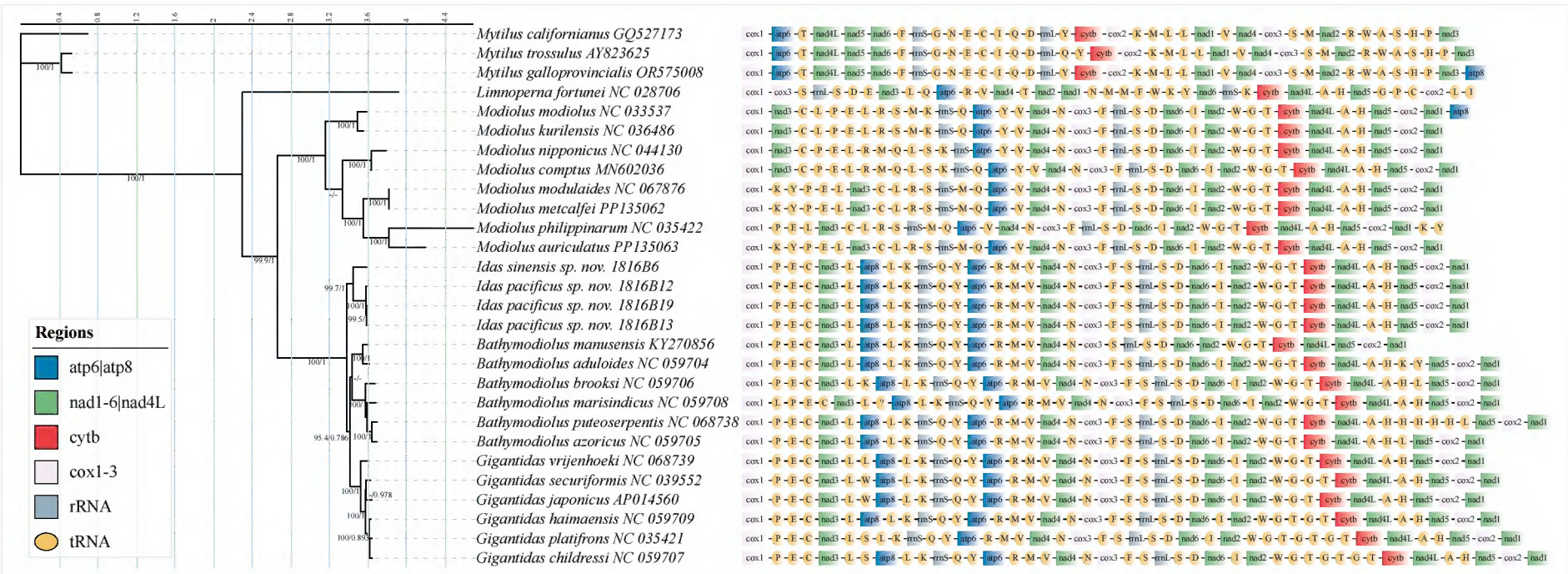

Figure 2. Mitophylogenyinferred using ML and BI methods (based on the concatenated dataset of 12 PCGs and 2 rRNA genes) and gene order for the family Mytilidae. Numbers near the nodes represent ML bootstrap values and BI posterior probabilities (only values >75% and >0.75 are shown, respectively).

area. Shells resemble those of *I. iwaotakii*, but overall outline more elliptical compared to *I. iwaotakii* due to more similar anterior and posterior heights.

Shell morphology. Shells 9.3 mm to 13.4 mm in length, 3.1 mm to 3.9 mm in height (Fig. 3H–I), thin, fragile, deep olive-yellow, semi-transparent, very thin nacreous layer. Highly elongated, elliptical shape with concentric growth lines. Small specimen with rounded anterior and posterior margins; large specimen with broadly triangular posterior margins. Dorsal and ventral margins straight and nearly parallel, with slight incurvature along the ventral outline in larger specimens. Very short, dark brown bristles distributed mainly along the ridge from the posterior margin to the umbo. Umbo extremely anterior. Hinge plate slightly curved, with degenerated anterior hinge teeth (Fig. 4F–G). Inner shell surface smooth, lacking muscle scars. Prodissoconch pink and rounded.

Soft tissue anatomy. The soft tissue was poorly preserved to allow for detailed examination. However, the foot of the specimen preserved in alcohol was purple.

Gill-associated microbes. Only the gill tissues of the holotype (TIO2023-1816B6) could be used for analysis of symbiotic microbes. Among the bacteria associated with the gill, *Pseudohongiella* sp., *Reichenbachiella* sp., and SUP05 cluster were most abundant, representing 70%, 9%, and 7% of the sequences, respectively (Figs 5, 6A).

Habitat and distribution. So far, this species has only been found within wood. It is known only from the East China Sea (30.7°N, 127.8°E).

Etymology. The name *sinensis* – the Latinized form of China, refers to the type locality, within the Chinese EEZ of the East China Sea.

Remarks. *Idas sinensis* sp. nov. exhibits a close morphological and phylogenetic relationship with *I. iwaotakii*, as both species share an elongated shell shape, characterized by nearly parallel dorsal and ventral outlines, a feature that sets them apart from *Idas* species in other clades. The primary difference between these species (for specimens around 1 cm in length) lies in the curvature of the anterior and posterior margins: *Idas sinensis* sp. nov. has a more capsule-shaped outline, while *I. iwaotakii* has a more triangular profile.

Additionally, the Mediterranean species *Idas cristiani* Fr. Giusti, Mietto & Sbrana, 2012 and *Idas emmae* Fr. Giusti, Mietto & Sbrana, 2012 also exhibit an elongated form. However, none of the *Idas sinensis* sp. nov. specimens (9.3 mm and 13.4 mm) have anterior hinge teeth, whereas *I. cristiani* has 5–6 small teeth below the umbo, and *I. emmae* has three. Moreover, *Idas sinensis* sp. nov. has sparser bristles compared to *I. cristiani*, and its shell (H/L = 0.29–0.33) is higher than that of *I. emmae* (H/L = 0.25–0.26) (Giusti et al. 2012).

Idas pacificus sp. nov.

https://zoobank.org/18C6A39C-48B0-429F-803A-6A84CC33D358

Figs 3A–G, 4A–E, 7, 8A

(*Idas* sp. OTU-51 mentioned earlier; *Idas* sp. ESU D, as mentioned by Lorion et al. (2010))

Materials examined. All 23 specimens were collected from a piece of wood by trawling at 460–550 m seabed at 30.7°N, 127.8°E in April 2023.

Type material. ***Holotype*** • TIO2023-1816B14 (length: 10.8 mm); ***Paratypes*** • six specimens, TIO2023-1816B9, TIO2023-1816B12, TIO2023-1816B15, TIO2023-1816B24, TIO2023-1816B29, TIO2023-1816B30

Diagnosis. Adult specimens approximately measure 10 mm in length, resembling the general outline of *Idas ghisottii* Warén & Carrozza, 1990 from the Mediterranean region. Shells with an H/L ratio of about 0.36 to 0.45, maintaining a consistent overall shape across different sizes, though older individuals are slightly more elongated. Umbo located at approximately the anterior 1/7 to 1/9 of the shell length. The triangular area, from the posterior margin to the umbo, near the dorsal margin, is covered with bristles that match the external shell surface color. The base of the bristles is triangular in shape.

Shell morphology. Shells 3.2–10.8 mm in length, 1.4–4.1 mm in height (Fig. 3A–G). Shells thin, olive-yellow,

Figure 3. Specimen photographs of *Idas pacificus* sp. nov. and *Idas sinensis* sp. nov. **A–G.** *Idas pacificus* sp. nov.: **A.** Sample ID: TIO2023-1816B30, paratype, left valve; **B.** Sample ID: TIO2023-1816B29, paratype, left valve; **C.** Sample ID: TIO2023-1816B24, paratype, left valve; **C'.** Dorsal view; **D.** Sample ID: TIO2023-1816B9, paratype, left valve; **E.** Sample ID: TIO2023-1816B12, paratype, left valve; **F.** Sample ID: TIO2023-1816B15, paratype, left valve; **G.** Sample ID: TIO2023-1816B14, holotype, left & right valve; **G'.** Dorsal view; **H, I.** *Idas sinensis* sp. nov.: **H.** TIO2023-1816B21, paratype, left valve; **I.** TIO2023-1816B6, holotype, left & right valve; **I'.** Dorsal view. Scale bar: 2 mm.

semi-transparent, with prominent concentric growth lines. Shells oval, with straight dorsal margin, slightly incurved ventral outline, and rounded posterior margin. Triangular area near dorsal margin, from posterior margin to umbo, sparsely covered with bristles. Umbo located at approximately the anterior 1/7 to 1/9, shifting forward with increasing shell size and tilting slightly forward. Hinge plate slender and straight (Fig. 4A–E). Both inner and outer shell surfaces with pearly luster. Inner shell surface smooth, faint traces of anterior adductor scar and pallial line, difficult to discern under optical microscope. Posterior adductor scar large, nearly circular; anterior adductor scar shallow, curved droplet-shaped (SEM images in Fig. 7C). Pallial sinus indentation small. Prodissoconch pink, rounded, smooth, ~400 µm in diameter.

Soft tissue anatomy. Foot well-developed, approximately 40% of shell length (Fig. 7). Like *I. macdonaldi*, byssal retractors continuous and not divided into posterior and anterior portions (Gustafson et al. 1998). Byssus retractor muscle and pedal retractor muscle fused into a single strand. Cross-section of anterior adductor muscle teardrop-shaped, posterior adductor muscle round. No byssus observed.

Gill-associated microbes. The 13 specimens of *Idas pacificus* sp. nov. share 11 common microbial species

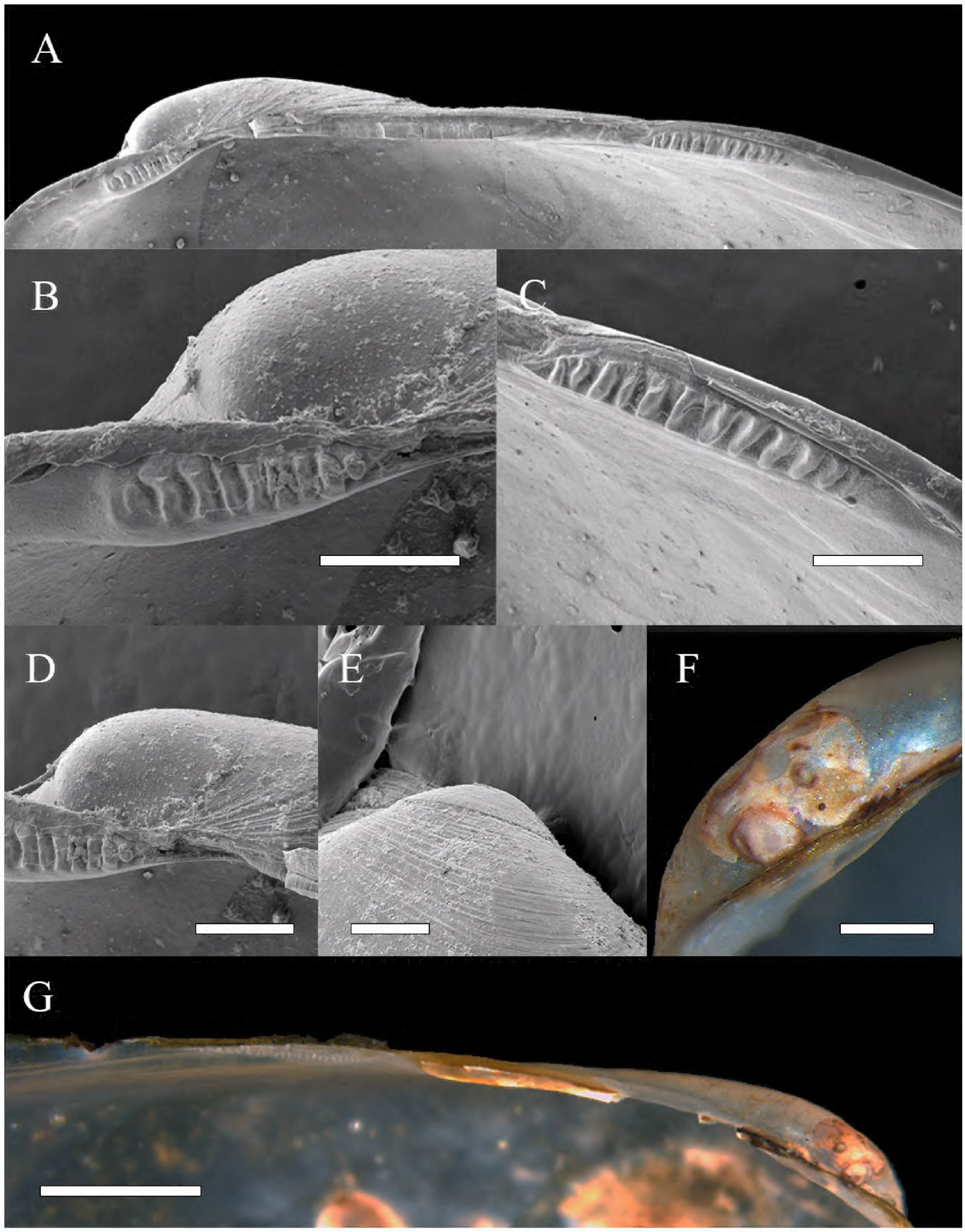

Figure 4. Photographs of the hinge structures and prodissoconch of the specimens of *Idas pacificus* sp. nov. and *Idas sinensis* sp. nov. **A–E.** *Idas pacificus* sp. nov. Sample ID: TIO2023-1816B7, length: 8.3 mm. **A.** Hinge line of specimen; **B.** Hinge denticles located immediately below the umbo; **C.** Hinge denticles located posterior of the ligament; **D.** Prodissoconch; **E.** Ventral view of the larval shell (left valve); **F, G.** *Idas sinensis* sp. nov. Sample ID: TIO2023-1816B6, length: 9.3 mm. hinge line of specimen; **F.** Prodissoconch; **G.** Hinge line of specimen (left valve). Scale bars: 200 µm (**B–E**); 500 µm (**F**); 1 mm (**G**).

(Fig. 6), with 7 of these accounting for more than 1% of the total read abundance. Specifically, three species belong to Gammaproteobacteria, two to Bacteroidia, and two to Campylobacteria. In addition, genetic diversity among symbionts from different *Idas pacificus* sp. nov. specimens is notable, with 11 different SUP05 cluster genotypes detected among the 13 specimens (Fig. 5). ASV2 is the most common SUP05 genotype, dominating in 6 of the specimens where it accounts for over 50% of all SUP05 sequences. In the remaining specimens, the predominant SUP05 genotypes include ASV4, ASV10, ASV96, ASV144, and ASV325.

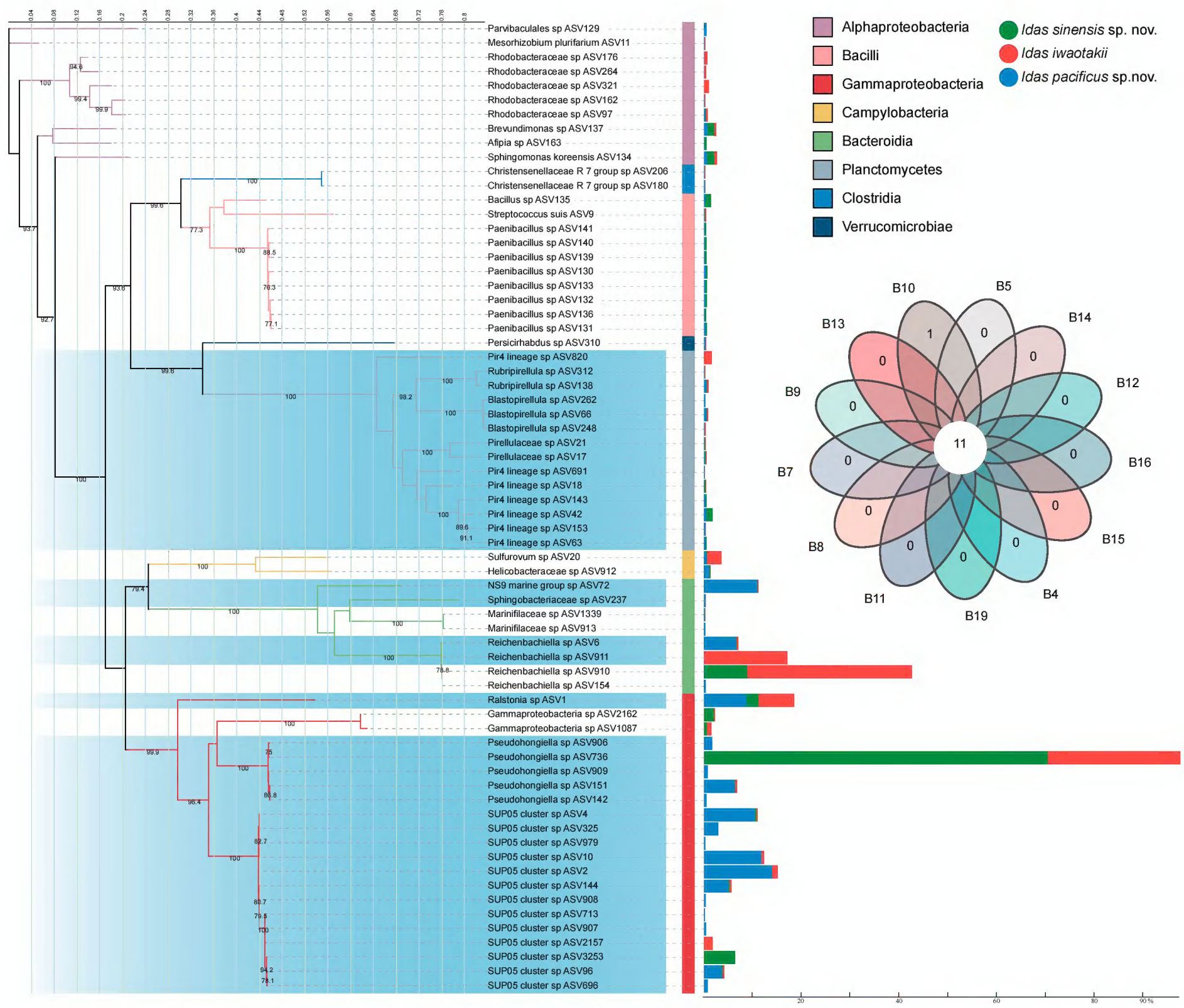

Figure 5. The ML phylogenetic tree of gill-associated microbiota from 16 *Idas* samples obtained in this study. Numbers near the nodes represent bootstrap values (only values >75% are shown). Branches with a blue background indicate bacterial species shared by 13 *Idas pacificus* sp. nov. samples. Stacked bar chart adjacent to the phylogenetic tree shows the relative abundance of each ASV in different species (expressed as the percentage of sequences averaged per individual). Venn diagram displays the symbiont species shared among the 13 *Idas pacificus* sp. nov. individuals.

Habitat and distribution. The *Idas pacificus* sp. nov. specimens lived inside holes in a piece of sunken wood. These holes are typically round, each containing only a single individual. Unlike those of *I. iwaotakii* and *Idas sinensis* sp. nov., the holes occupied by *I. pacificus* sp. nov. are black (Fig. 8A), which may be due to FeS precipitation (Bienhold et al. 2013). This hypothesis is supported by the functional heatmap of the microbes recovered from the gill tissues (Fig. 6B), which showed that *I. pacificus* sp. nov. had a high abundance of sulfur-oxidizing bacteria. Due to the limited samples of *I. iwaotakii* and *Idas sinensis* sp. nov. and the fact that all analyzed *Idas* samples came from the same piece of wood, we could not determine the generality of this phenomenon.

The type specimens were collected from sunken wood in the East China Sea at depths of approximately 460–550 meters. *Idas pacificus* sp. nov. was reported on sunken wood in Philippines and Vanuatu as *Idas* sp. ESU D by Lorion et al. (2009), and experimental bones placed in Japanese waters (Lorion et al. 2013). Comparing our DNA barcode data for *Idas pacificus* sp. nov. with those available on GenBank indicates that it is conspecific to *Idas* sp. ESU D (GenBank Acc. No. HF545116, EU702350, EU350071, EU702358), with K2P distances of 0–0.3%, being smaller than the inter-specific genetic divergence between other species of *Idas* (e.g. 19.8% between *I. argenteus* and *I. washingtonia*, and 2.8% between *I. macdonaldi* and *I. modiolaeformis*, See Suppl. material 8 for details.). Therefore, *Idas pacificus* sp. nov. may be widespread in the Western Pacific, including East China Sea (this study), Santo Island in Vanuatu (Lorion et al. 2009), Bohol Sea (Duperron et al. 2009), and Japanese waters (Lorion et al. 2013), with water depth ranging from 460 to 1764 meters (Duperron et al. 2009; Lorion et al. 2013).

Etymology. Since our comparison with DNA barcode data obtained from GenBank indicates this species

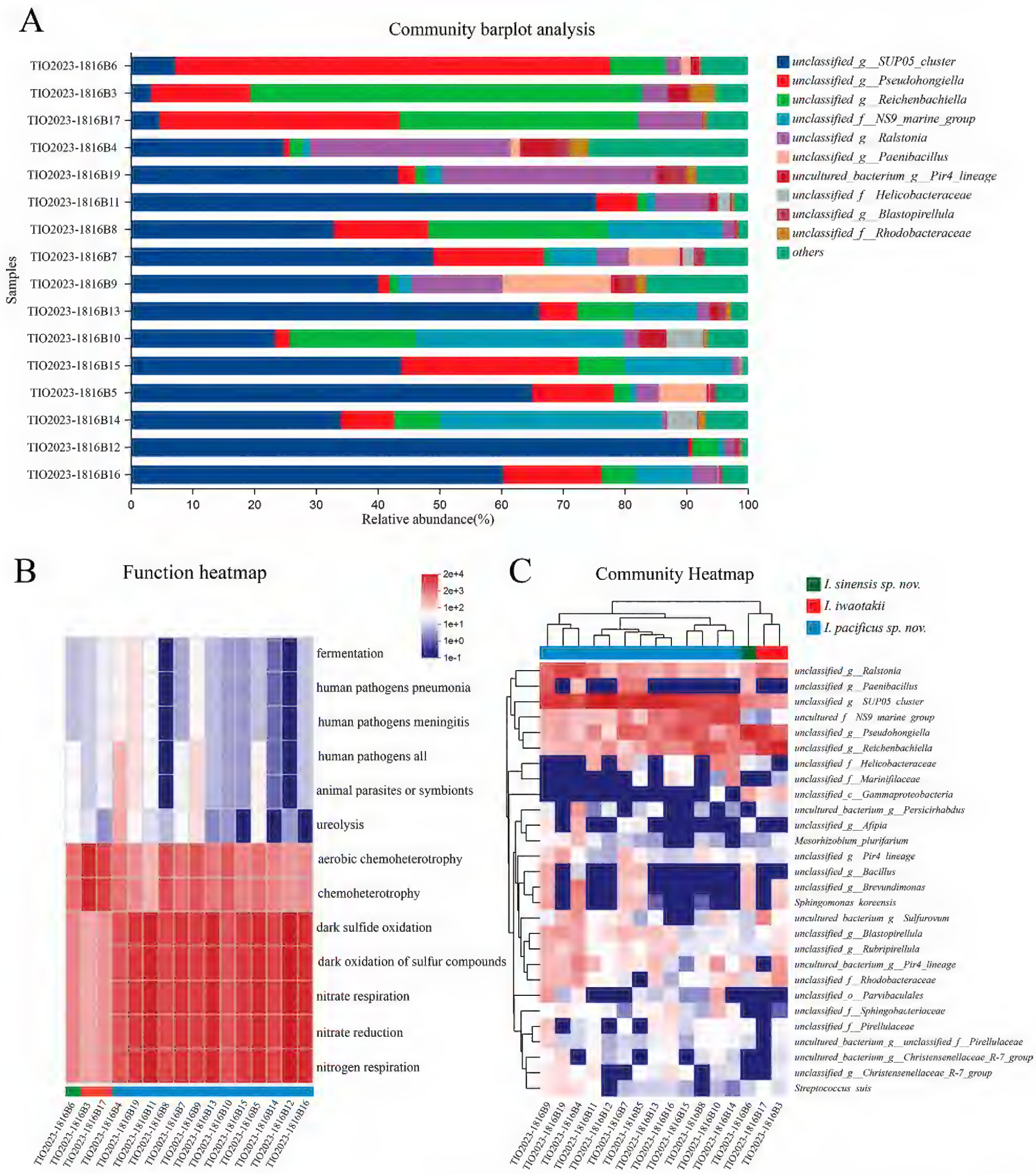

Figure 6. Gill-associated Bacterial Community Analysis of *Idas*. **A.** Relative abundance; **B.** Functional heatmap generated by FAPROTAX; **C.** Community heatmap.

to be widely distributed in the Western Pacific, the name "*pacificus*" was given to the species.

Remarks. *Idas pacificus* sp. nov. is notably different from *I. iwaotakii*, which has a very elongated shape, a sharply pointed posterior margin, and shorter and darker bristles that appear to degrade with increasing size. Bristles are also a key distinguishing feature that separates this species from *I. washingtonius*, *I. coppingeri*, and *I. indicus*. The first two species lack bristles (Murray et al. 1885; Harbo and Gillespie 2021), while *I. indicus* has very short bristles and a more pronounced curvature of the ventral outline (Smith 1899).

Adaptation of *Idas pacificus* sp. nov. and *Idas sinensis* sp. nov. to the sunken wood habitat

Sunken wood provides shelter for a variety of marine organisms, offering both a carbon source and substrate (Altamia et al. 2024). Compared to other Bathymodiolinae species

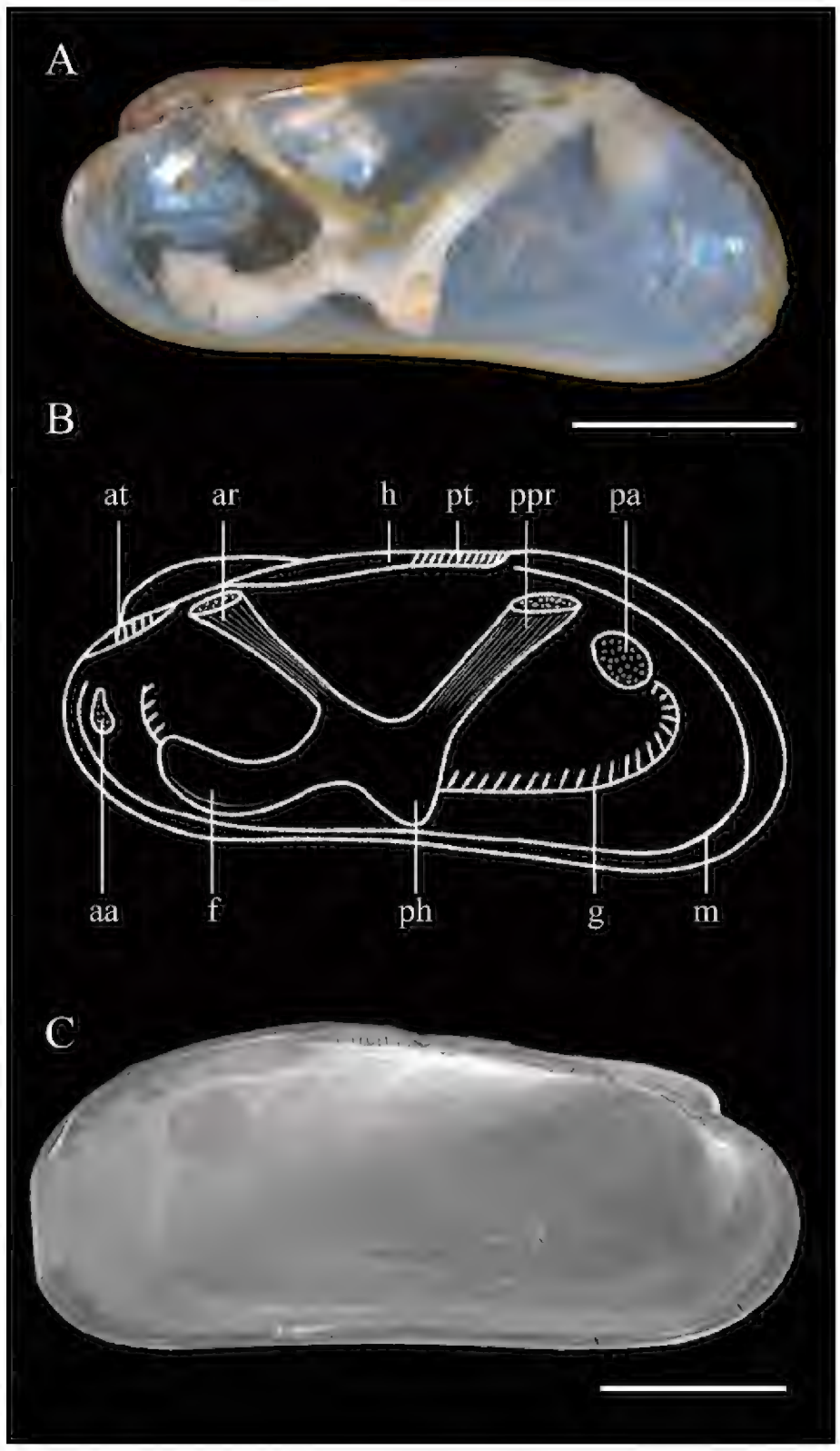

Figure 7. Internal View of *Idas pacificus* sp. nov. **A.** Sample ID: TIO2023-1816B9, lateral view; **B.** Schematic drawing of the right shell and internal structures based on TIO2023-1816B9, the positions of the gill and mantle confirmed across multiple samples; **C.** SEM image showing the anterior adductor scar, pallial line, posterior adductor scar, and pallial sinus, sample ID: TIO2023-1816B7. Note that the posterior margin of the specimen is incomplete. Abbreviations: aa: anterior adductor; ar: anterior byssus retractor; at: anterior hinge teeth; f: foot; g: gill; h: hinge; m: mantle; pa: posterior adductor; ph: pedal heel; ppr: posterior byssus retractor and pedal retractor; pt: posterior hinge teeth. Scale bars: 2 mm.

Figure 8. Situ views of the **A.** *Idas pacificus* sp. nov. and **B.** *I iwaotakii*. Both images show the specimens with portions of the wood removed to expose them. Scale bars: 2mm.

inhabiting hydrothermal vents and cold seeps, mussels associated with organic fall ecosystems are generally smaller in size. While hydrothermal vents and cold seeps can vary in size and longevity – ranging from small, short-lived outgassing sites to areas spanning several million square meters (Andrianasolo et al. 2012; Wang et al. 2022), wood fall habitats are typically more localized and transient. Organisms inhabiting these transient environments may need to complete their life cycles within a limited timeframe, and smaller body sizes could represent an adaptation to such constraints.

Both *Idas pacificus* sp. nov. and *Idas sinensis* sp. nov. have thin and fragile shells, which would offer little protection against predators in more exposed environments. However, the sunken wood provides a natural shielding habitat. Altamia et al. (2024) suggested that the bristles of *Idas* species may help keep the valves away from the burrow walls and possibly improve water flow around the animals. This hypothesis may partially explain the differences in bristle development between the two species. *Idas pacificus* sp. nov., with its shorter and more triangular body shape, exhibits more developed bristles, which may enhance stability in cylindrical burrows. Notably, neither species exhibited byssal threads, likely an adaptation to inhabiting wood holes where strong water currents are not a concern.

Diversity of gill-associated microbes

Sample TIO2023-1816B18 was excluded from further analysis due to substantially fewer valid sequences (7,614, compared to > 18,000 in each of the other 16 specimens). A total of 2,853 ASVs were generated across all samples, with an average sequence length of 1,496 bp. After removing chloroplast and mitochondrial sequences and those with an abundance below 0.001, 28 species remained, encompassing 68 ASVs.

We compared the gill-associated bacterial community composition among *Idas pacificus* sp. nov., *I. iwaotakii* and *Idas sinensis* sp. nov. obtained in this study (Figs 5, 6C). All three species harbor *Reichenbachiella*

sp., *Pseudohongiella* sp., and species of the SUP05 cluster in their gills, but the relative abundance and the number of ASVs of these bacteria differ among the three species. Four *Reichenbachiella* sp. ASVs were detected in this study (Fig. 5), with only ASV6 found in *Idas pacificus* sp. nov. and ASV911 exclusively in *I. iwaotakii*. For *Pseudohongiella* sp., its relative abundance reached 30% in *I. iwaotakii* and 70% in *I. sinensis* sp. nov. samples, with ASV736 comprising over 95% of all *Pseudohongiella* sp. sequences in these two species. In contrast, the relative abundance of *Pseudohongiella* sp. in *Idas pacificus* sp. nov. samples was only around 10%, and the proportion of ASV736 sequences was less than 1%.

In *Idas sinensis* sp. nov., the most abundant bacterium is *Pseudohongiella* sp. This bacterium was present in all *Idas* samples examined in this study and showed high relative abundance in the gills of the closely related *I. iwaotakii*. Therefore, we hypothesize that it is likely a gill symbiont of *Idas sinensis* sp. nov. However, since only one specimen was examined for gill-associated bacteria, it remains unclear whether the less abundant bacteria are random associates or symbionts.

In the 14 *Idas pacificus* sp. nov. samples, the relative abundance of the chemosynthetic SUP05 group ranges from 23% to 90%, while in *I. iwaotakii* and *I. sinensis* sp. nov. samples, the maximum relative abundance of the SUP05 group is only 7% (Fig. 6A). Although the SUP05 group is detected in the gills of all three species, there is a marked difference in the dominant ASVs. In *I. iwaotakii*, ASV2157 is the dominant ASV and is found exclusively in this species, while in *I. sinensis* sp. nov., ASV3253 is the dominant ASV and is also unique to this species.

The presence of the same bacterial species, especially those of the chemosynthetic SUP05 group, across different *Idas* species suggests that these are potential symbionts playing crucial roles in the survival of *Idas*. Given that there is substantial evidence indicating that bathymodioline symbionts are primarily acquired through horizontal transmission (Won et al. 2008; Kiel 2010; Romero Picazo et al. 2019; Franke et al. 2021; Lin et al. 2022) and that the piece of wood was only 35 cm long, the likelihood of uneven bacterial distribution due to water flow is minimal. We speculate that different host species may exhibit a preference for specific genotypes of symbionts, or the host may acquire symbionts before colonizing the sunken wood, with genetic differences in the same symbiont species among different *Idas* species arising from bacteria in distinct water masses encountered during the planktonic phase. The variation in the relative abundance of SUP05 may suggest that microbial communities play different roles in different *Idas* hosts.

The SUP05 cluster dominated the gill-associated bacterial community of *Idas pacificus* n. sp. (Figs 5, 6A). These species have been known to be chemosynthetic, obtaining energy through sulfur oxidation (Duperron et al. 2008b) and are common in bathymodiolines, including those of the genera *Idas* (Duperron et al. 2008b), *Adipicola* (Fujiwara et al. 2010), *Nypamodiolus* (Lin et al. 2022) and *Bathymodiolus* (van der Heijden et al. 2012; Raggi et al. 2013).

The function heatmap (Fig. 6B) reveals that, compared to *Idas iwaotakii* and *Idas sinensis* sp. nov., the symbiotic microbes in the gills of *Idas pacificus* sp. nov. show a higher nitrogen and sulfur metabolic potential. By contrast, the symbionts of *I. iwaotakii* exhibit a stronger association with aerobic and general chemoheterotrophy, with *Idas sinensis* sp. nov. showing an intermediate profile. The differences in the relative abundance of SUP05 among different hosts may be a key factor contributing to this variation, as this group can couple sulfide oxidation with nitrate reduction (Callbeck et al. 2018).

The community heatmap (Fig. 6C) also shows a high correlation in bacterial composition between *Idas iwaotakii* and *Idas sinensis* sp. nov. Given that these two species are closely related phylogenetically, their preference for specific bacteria may stem from a shared ancestral lineage. The differentiation in symbiotic microbes among the *Idas* individuals from the same piece of sunken wood could suggest niche differentiation among closely related hosts. However, considering the observed flexibility in symbiont composition among *Idas* species (Duperron et al. 2008a; Rodrigues et al. 2015), the limited number of samples for *Idas iwaotakii* and *Idas sinensis* sp. nov., and the fact that our specimens originated from the same piece of wood, it remains unclear if the symbiont community of these two new species varies with habitat. Further studies are required to investigate these inter- and intra-species variations.

Conclusion

This study describes two new species from sunken wood habitats on the East China Sea: *Idas sinensis* sp. nov. and *Idas pacificus* sp. nov., detailing their morphological characteristics. These findings extend the known distribution and diversity of chemosynthetic mussels. For the first time, we present mitochondrial genome sequences of the *Idas* species and determine their phylogenetic relationships with other bathymodioline mussels. Our results confirm that these mussels from sunken wood are closely related to their counterparts from cold seeps and hydrothermal vents in the *Gigantidas* and *Bathymodiolus* genera. Additionally, we obtained full-length 16S rRNA sequences of the gill-associated bacteria from *I. pacificus* sp. nov., *I. sinensis* sp. nov., and *I. iwaotakii*. Significant differences were observed in the composition of gill symbionts among these species, potentially reflecting ecological niche differentiation. Collectively, our findings highlight the close evolutionary and symbiotic relationships between sunken wood mussels and other chemosynthetic mussels.

Data availability statement

All gene sequences generated in this study have been deposited in the GenBank database under the accession numbers listed in Suppl. material 6.

Acknowledgements

We sincerely thank the anonymous reviewer for their valuable comments, which have greatly benefited our work. For assistance with the identification of sea urchins in the sunken wood fauna, we are grateful to Professor Rich Mooi, Curator Emeritus at the California Academy of Sciences. We acknowledge the financial support provided by the National Key Research and Development Program of China (2022–24, 2022YFC2804001), the Natural Science Foundation of Fujian Province, China (2023J011373), and the Natural Science Foundation of Xiamen, China (3502Z20227252), and the General Research Fund of Hong Kong (12101021).

References

Altamia MA, Appiah-Madson HJ, Falco-Poulin R, Huettel B, Rubin-Blum M, Dubilier N, Gruber-Vodicka HR, Leisch N, Distel DL (2024) Wooden steps to shallow depths: A new bathymodiolin mussel, *Vadumodiolus teredinicola*, inhabits shipworm burrows in an ancient submarine forest. Deep Sea Research Part I: Oceanographic Research Papers 204: 104220. https://doi.org/10.1016/j.dsr.2023.104220

Andrews S (2010) FastQC: a quality control tool for high throughput sequence data. Cambridge, United Kingdom.

Andrianasolo E, Lutz R, Falkowski P (2012) Deep-sea hydrothermal vents as a new source of drug discovery. Studies in Natural Products Chemistry 36: 43–66. https://doi.org/10.1016/B978-0-444-53836-9.00020-7

Anisimova M, Gil M, Dufayard J-F, Dessimoz C, Gascuel O (2011) Survey of branch support methods demonstrates accuracy, power, and robustness of fast likelihood-based approximation schemes. Systematic Biology 60: 685–699. https://doi.org/10.1093/sysbio/syr041

Baco-Taylor AR (2002) Food web structure, succession, and phylogenetics on deep-sea whale skeletons. University of Hawai'i at Manoa.

Bernardino AF, Smith CR, Baco A, Altamira I, Sumida PY (2010) Macrofaunal succession in sediments around kelp and wood falls in the deep NE Pacific and community overlap with other reducing habitats. Deep Sea Research Part I: Oceanographic Research Papers 57: 708–723. https://doi.org/10.1016/j.dsr.2010.03.004

Bienhold C, Pop Ristova P, Wenzhöfer F, Dittmar T, Boetius A (2013) How deep-sea wood falls sustain chemosynthetic life. PLoS One 8: e53590. https://doi.org/10.1371/journal.pone.0053590

Callahan B (2022) DADA2: Fast and accurate sample inference from amplicon data with single-nucleotide resolution (1.16).

Callbeck CM, Lavik G, Ferdelman TG, Fuchs B, Gruber-Vodicka HR, Hach PF, Littmann S, Schoffelen NJ, Kalvelage T, Thomsen S (2018) Oxygen minimum zone cryptic sulfur cycling sustained by offshore transport of key sulfur oxidizing bacteria. Nature Communications 9: 1729. https://doi.org/10.1038/s41467-018-04041-x

Chan PP, Lin BY, Mak AJ, Lowe TM (2021) tRNAscan-SE 2.0: improved detection and functional classification of transfer RNA genes. Nucleic Acids Research 49: 9077–9096. https://doi.org/10.1093/nar/gkab688

Chen S, Zhou Y, Chen Y, Gu J (2018) fastp: an ultra-fast all-in-one FASTQ preprocessor. Bioinformatics 34: i884–i890. https://doi.org/10.1093/bioinformatics/bty560

Danecek P, Bonfield JK, Liddle J, Marshall J, Ohan V, Pollard MO, Whitwham A, Keane T, McCarthy SA, Davies RM (2021) Twelve years of SAMtools and BCFtools. Gigascience 10: giab008. https://doi.org/10.1093/gigascience/giab008

DeLeo DM, Morrison CL, Sei M, Salamone V, Demopoulos AW, Quattrini AM (2022) Genetic diversity and connectivity of chemosynthetic cold seep mussels from the US Atlantic margin. BMC Ecology and Evolution 22: 76. https://doi.org/10.1186/s12862-022-02027-4

Distel DL, Baco AR, Chuang E, Morrill W, Cavanaugh C, Smith CR (2000) Do mussels take wooden steps to deep-sea vents? Nature 403: 725–726. https://doi.org/10.1038/35001667

Doucet-Beaupré H, Breton S, Chapman EG, Blier PU, Bogan AE, Stewart DT, Hoeh WR (2010) Mitochondrial phylogenomics of the Bivalvia (Mollusca): searching for the origin and mitogenomic correlates of doubly uniparental inheritance of mtDNA. BMC Evolutionary Biology 10: 1–19. https://doi.org/10.1186/1471-2148-10-50

Duperron S, Halary S, Lorion J, Sibuet M, Gaill F (2008a) Unexpected co-occurrence of six bacterial symbionts in the gills of the cold seep mussel *Idas* sp. (Bivalvia: Mytilidae). Environmental Microbiology 10: 433–445. https://doi.org/10.1111/j.1462-2920.2007.01465.x

Duperron S, Laurent MC, Gaill F, Gros O (2008b) Sulphur-oxidizing extracellular bacteria in the gills of Mytilidae associated with wood falls. FEMS Microbiology Ecology 63: 338–349. https://doi.org/10.1111/j.1574-6941.2008.00438.x

Duperron S, Lorion J, Samadi S, Gros O, Gaill F (2009) Symbioses between deep-sea mussels (Mytilidae: Bathymodiolinae) and chemosynthetic bacteria: diversity, function and evolution. Comptes Rendus Biologies 332: 298–310. https://doi.org/10.1016/j.crvi.2008.08.003

Franke M, Geier B, Hammel JU, Dubilier N, Leisch N (2021) Coming together – symbiont acquisition and early development in deep-sea bathymodioline mussels. Proceedings of the Royal Society B: Biological Sciences 288: 20211044. https://doi.org/10.1098/rspb.2021.1044

Fujiwara Y, Kawato M, Noda C, Kinoshita G, Yamanaka T, Fujita Y, Uematsu K, Miyazaki J-I (2010) Extracellular and mixotrophic symbiosis in the whale-fall mussel *Adipicola pacifica*: a trend in evolution from extra-to intracellular symbiosis. PLoS One 5: e11808. https://doi.org/10.1371/journal.pone.0011808

Fukasawa Y, Kobayashi-Iwatani H, Kawato M, Kobayashi H, Fujiwara Y, Miyazaki J-I (2015) Dispersal ability and genetic structure in Mytilid mussels of whale-fall communities. Open Journal of Marine Science 5: 295–305. https://doi.org/10.4236/ojms.2015.53025

Genio L, Kiel S, Cunha MR, Grahame J, Little CT (2012) Shell microstructures of mussels (Bivalvia: Mytilidae: Bathymodiolinae) from deep-sea chemosynthetic sites: Do they have a phylogenetic significance? Deep Sea Research Part I: Oceanographic Research Papers 64: 86–103. https://doi.org/10.1016/j.dsr.2012.02.002

Genio L, Rodrigues CF, Guedes IF, Almeida H, Duperron S, Hilario A (2015) Mammal carcasses attract a swarm of mussels in the deep Atlantic: insights into colonization and biogeography of a chemosymbiotic species. Marine Ecology 36: 71–81. https://doi.org/10.1111/maec.12217

Giusti F, Mietto P, Sbrana C (2012) Il genere *Idas* (Mytilidae, Bathymodiolinae) in Mediterraneo, con la descrizione di quattro nuove specie. Bollettino Malacologico: 122–135.

Grant JR, Enns E, Marinier E, Mandal A, Herman EK, Chen C-y, Graham M, Van Domselaar G, Stothard P (2023) Proksee: in-depth characterization and visualization of bacterial genomes. Nucleic Acids Research 51: W484–W492. https://doi.org/10.1093/nar/gkad326

Guindon S, Dufayard J-F, Lefort V, Anisimova M, Hordijk W, Gascuel O (2010) New algorithms and methods to estimate maximum-likelihood phylogenies: assessing the performance of PhyML 3.0. Systematic Biology 59: 307–321. https://doi.org/10.1093/sysbio/syq010

Gustafson RG, Turner RD, Lutz RA, Vrijenhoek RC (1998) A new genus and five new species of mussels (Bivalvia, Mytilidae) from deep-sea sulfide/hydrocarbon seeps in the Gulf of Mexico. Malacologia 40: 63–112.

Harbo R, Gillespie G (2021) A northern range extension of the Washington combmussel, *Idas washingtonius* (Bernard, 1978). The Dredgings 61: 3–4.

Jeffreys JG (1876) XLII. – New and peculiar mollusca of the Pecten, Mytilus, and Arca families procured in the 'Valorous' Expedition. Journal of Natural History 18: 424–436. https://doi.org/10.1080/00222937608682068

Kalyaanamoorthy S, Minh BQ, Wong TK, Von Haeseler A, Jermiin LS (2017) ModelFinder: fast model selection for accurate phylogenetic estimates. Nature Methods 14: 587–589. https://doi.org/10.1038/nmeth.4285

Katoh K, Standley DM (2013) MAFFT multiple sequence alignment software version 7: improvements in performance and usability. Molecular Biology and Evolution 30: 772–780. https://doi.org/10.1093/molbev/mst010

Kiel S (2010) The vent and seep biota: aspects from microbes to ecosystems. Vol. 33, Springer Science & Business Media. https://doi.org/10.1007/978-90-481-9572-5

Kimball RT, Guido M, Hosner PA, Braun EL (2021) When good mitochondria go bad: Cyto-nuclear discordance in landfowl (Aves: Galliformes). Gene 801: 145841. https://doi.org/10.1016/j.gene.2021.145841

Kyuno A, Shintaku M, Fujita Y, Matsumoto H, Utsumi M, Watanabe H, Fujiwara Y, Miyazaki J-I (2009) Dispersal and differentiation of deep-sea mussels of the genus *Bathymodiolus* (Mytilidae, Bathymodiolinae). Journal of Marine Sciences 2009: 625672. https://doi.org/10.1155/2009/625672

Lanfear R, Frandsen PB, Wright AM, Senfeld T, Calcott B (2017) PartitionFinder 2: new methods for selecting partitioned models of evolution for molecular and morphological phylogenetic analyses. Molecular Biology and Evolution 34: 772–773. https://doi.org/10.1093/molbev/msw260

Lee Y, Kwak H, Shin J, Kim S-C, Kim T, Park J-K (2019) A mitochondrial genome phylogeny of Mytilidae (Bivalvia: Mytilida). Molecular Phylogenetics and Evolution 139: 106533. https://doi.org/10.1016/j.ympev.2019.106533

Letunic I, Bork P (2021) Interactive Tree Of Life (iTOL) v5: an online tool for phylogenetic tree display and annotation. Nucleic Acids Research 49: W293–W296. https://doi.org/10.1093/nar/gkab301

Li H (2013) Aligning sequence reads, clone sequences and assembly contigs with BWA-MEM. arXiv 1303.3997:

Li Y-X, Sun Y, Lin Y-T, Xu T, Ip JCH, Qiu J-W (2023) Cold seep macrofauna. In: South China Sea Seeps. Springer Nature Singapore Singapore, 69–88. https://doi.org/10.1007/978-981-99-1494-4_5

Lin Y-T, Kiel S, Xu T, Qiu J-W (2022) Phylogenetic placement, morphology and gill-associated bacteria of a new genus and species of deep-sea mussel (Mytilidae: Bathymodiolinae) from the South China Sea. Deep Sea Research Part I: Oceanographic Research Papers 190: 103894. https://doi.org/10.1016/j.dsr.2022.103894

Liu J, Liu H, Zhang H (2018) Phylogeny and evolutionary radiation of the marine mussels (Bivalvia: Mytilidae) based on mitochondrial and nuclear genes. Molecular Phylogenetics and Evolution 126: 233–240. https://doi.org/10.1016/j.ympev.2018.04.019

Lorion J, Samadi S (2010) Species richness, sampling bias and phylogenetics in deep-sea mussels. Cahiers de Biologie Marine 51: 435.

Lorion J, Duperron S, Gros O, Cruaud C, Samadi S (2009) Several deep-sea mussels and their associated symbionts are able to live both on wood and on whale falls. Proceedings of the Royal Society B: Biological Sciences 276: 177–185. https://doi.org/10.1098/rspb.2008.1101

Lorion J, Buge B, Cruaud C, Samadi S (2010) New insights into diversity and evolution of deep-sea Mytilidae (Mollusca: Bivalvia). Molecular Phylogenetics and Evolution 57: 71–83. https://doi.org/10.1016/j.ympev.2010.05.027

Lorion J, Halary S, Do Nascimento J, Samadi S, Couloux A, Duperron S (2012) Evolutionary history of *Idas* sp. Med, (Bivalvia: Mytilidae), a cold seep mussel bearing multiple symbionts. Cahiers de Biologie Marine 53(1): 77–87.

Lorion J, Kiel S, Faure B, Kawato M, Ho SY, Marshall B, Tsuchida S, Miyazaki J-I, Fujiwara Y (2013) Adaptive radiation of chemosymbiotic deep-sea mussels. Proceedings of the Royal Society B: Biological Sciences 280: 20131243. https://doi.org/10.1098/rspb.2013.1243

Louca S, Parfrey LW, Doebeli M (2016) Decoupling function and taxonomy in the global ocean microbiome. Science 353: 1272–1277. https://doi.org/10.1126/science.aaf4507

McArthur A, Tunnicliffe V (1998) Relics and antiquity revisited in the modern vent fauna. Geological Society, London, Special Publications 148: 271–291. https://doi.org/10.1144/GSL.SP.1998.148.01.15

McCowin MF, Feehery C, Rouse GW (2020) Spanning the depths or depth-restricted: three new species of Bathymodiolus (Bivalvia, Mytilidae) and a new record for the hydrothermal vent Bathymodiolus thermophilus at methane seeps along the Costa Rica margin. Deep Sea Research Part I: Oceanographic Research Papers 164: 103322. https://doi.org/10.1016/j.dsr.2020.103322

McGuire JA, Linkem CW, Koo MS, Hutchison DW, Lappin AK, Orange DI, Lemos-Espinal J, Riddle BR, Jaeger JR (2007) Mitochondrial introgression and incomplete lineage sorting through space and time: phylogenetics of crotaphytid lizards. Evolution 61: 2879–2897. https://doi.org/10.1111/j.1558-5646.2007.00239.x

Meng G, Li Y, Yang C, Liu S (2019) MitoZ: a toolkit for animal mitochondrial genome assembly, annotation and visualization. Nucleic Acids Research 47: e63–e63. https://doi.org/10.1093/nar/gkz173

Meyer CP (2003) Molecular systematics of cowries (Gastropoda: Cypraeidae) and diversification patterns in the tropics. Biological Journal of the Linnean Society 79: 401–459. https://doi.org/10.1046/j.1095-8312.2003.00197.x

Mietto P, Quaggiotto E, Giusti F, Sbrana C (2019) Taxonomic and nomenclatural notes on the genus *Idas* (Bivalvia: Mytilidae). Bollettino Malacologico 55: 116–125.

Murray J, Thomson CW, Nares GS, Thomson FT (1885) Report on the scientific results of the voyage of HMS Challenger during the years 1873–76 under the command of Captain George S. Nares and the late Captain Frank Tourle Thomson. Vol. 2,HM Stationery Office. https://doi.org/10.5962/bhl.title.109677

Nawrocki EP, Eddy SR (2013) Infernal 1.1: 100-fold faster RNA homology searches. Bioinformatics 29: 2933–2935. https://doi.org/10.1093/bioinformatics/btt509

Newman WA (1985) The abyssal hydrothermal vent invertebrate fauna. A glimpse of antiquity? Bulletin of the Biological Society of Washington 6: 231– 242.

Nguyen L-T, Schmidt HA, Von Haeseler A, Minh BQ (2015) IQ-TREE: a fast and effective stochastic algorithm for estimating maximum-likelihood phylogenies. Molecular Biology and Evolution 32: 268–274. https://doi.org/10.1093/molbev/msu300

Olu-Le Roy K, Von Cosel R, Hourdez S, Carney S, Jollivet D (2007) Amphi-Atlantic cold-seep Bathymodiolus species complexes across the equatorial belt. Deep Sea Research Part I: Oceanographic Research Papers 54: 1890–1911. https://doi.org/10.1016/j.dsr.2007.07.004

Pailleret M, Haga T, Petit P, Privé-Gill C, Saedlou N, Gaill F, Zbinden M (2007) Sunken wood from the Vanuatu Islands: identification of wood substrates and preliminary description of associated fauna. Marine Ecology 28: 233–241. https://doi.org/10.1111/j.1439-0485.2006.00149.x

Pop Ristova P, Bienhold C, Wenzhöfer F, Rossel PE, Boetius A (2017) Temporal and spatial variations of bacterial and faunal communities associated with deep-sea wood falls. PLoS One 12: e0169906. https://doi.org/10.1371/journal.pone.0169906

Puillandre N, Lambert A, Brouillet S, Achaz G (2012) ABGD, Automatic Barcode Gap Discovery for primary species delimitation. Molecular ecology 21: 1864–1877. https://doi.org/10.1111/j.1365-294X.2011.05239.x

Rafinesque CS (1815) Analyse de la nature, ou tableau de l'univers et des corps organisés. Aux dépens de l'auteur. https://doi.org/10.5962/bhl.title.106607

Raggi L, Schubotz F, Hinrichs KU, Dubilier N, Petersen JM (2013) Bacterial symbionts of Bathymodiolus mussels and *Escarpia tubeworms* from Chapopote, an asphalt seep in the southern Gulf of Mexico. Environmental Microbiology 15: 1969–1987. https://doi.org/10.1111/1462-2920.12051

Ranwez V, Douzery EJ, Cambon C, Chantret N, Delsuc F (2018) MACSE v2: toolkit for the alignment of coding sequences accounting for frameshifts and stop codons. Molecular Biology and Evolution 35: 2582–2584. https://doi.org/10.1093/molbev/msy159

Rodrigues CF, Laming SR, Gaudron SM, Oliver G, Le Bris N, Duperron S (2015) A sad tale: has the small mussel *Idas argenteus* lost its symbionts? Biological Journal of the Linnean Society 114: 398–405. https://doi.org/10.1111/bij.12431

Romano C, Nunes-Jorge A, Le Bris N, Rouse GW, Martin D, Borowski C (2020) Wooden stepping stones: diversity and biogeography of deep-sea wood boring Xylophagaidae (Mollusca: Bivalvia) in the North-East Atlantic Ocean, with the description of a new genus. Frontiers in Marine Science 7: 579959. https://doi.org/10.3389/fmars.2020.579959

Romero Picazo D, Dagan T, Ansorge R, Petersen JM, Dubilier N, Kupczok A (2019) Horizontally transmitted symbiont populations in deep-sea mussels are genetically isolated. The ISME Journal 13: 2954–2968. https://doi.org/10.1038/s41396-019-0475-z

Ronquist F, Teslenko M, Van Der Mark P, Ayres DL, Darling A, Höhna S, Larget B, Liu L, Suchard MA, Huelsenbeck JP (2012) MrBayes 3.2: efficient Bayesian phylogenetic inference and model choice across a large model space. Systematic Biology 61: 539–542. https://doi.org/10.1093/sysbio/sys029

Rubinoff D, Cameron S, Will K (2006) A genomic perspective on the shortcomings of mitochondrial DNA for "barcoding" identification. Journal of Heredity 97: 581–594. https://doi.org/10.1093/jhered/esl036

Saccone C, De Giorgi C, Gissi C, Pesole G, Reyes A (1999) Evolutionary genomics in Metazoa: the mitochondrial DNA as a model system. Gene 238: 195–209. https://doi.org/10.1016/S0378-1119(99)00270-X

Samadi S, Quéméré E, Lorion J, Tillier A, von Cosel R, Lopez P, Cruaud C, Couloux A, Boisselier-Dubayle M-C (2007) Molecular phylogeny in mytilids supports the wooden steps to deep-sea vents hypothesis. Comptes Rendus Biologies 330: 446–456. https://doi.org/10.1016/j.crvi.2007.04.001

Samadi S, Puillandre N, Pante E, Boisselier MC, Corbari L, Chen WJ, Maestrati P, Mana R, Thubaut J, Zuccon D (2015) Patchiness of deep-sea communities in Papua New Guinea and potential susceptibility to anthropogenic disturbances illustrated by seep organisms. Marine Ecology 36: 109–132. https://doi.org/10.1111/maec.12204

Smith EA (1899) Natural history notes from HM Indian Marine Survey Steamer 'Investigator,'Commander TH Heming, RN – Series III., No. 1. On Mollusca from the Bay of Bengal and the Arabian Sea. Journal of Natural History 4: 11. https://doi.org/10.1080/00222939908678195

Talavera G, Castresana J (2007) Improvement of phylogenies after removing divergent and ambiguously aligned blocks from protein sequence alignments. Systematic Biology 56: 564–577. https://doi.org/10.1080/10635150701472164

Thubaut J, Corbari L, Gros O, Duperron S, Couloux A, Samadi S (2013a) Integrative biology of *Idas iwaotakii* (Habe, 1958), a 'model species' associated with sunken organic substrates. PLoS One 8: e69680. https://doi.org/10.1371/journal.pone.0069680

Thubaut J, Puillandre N, Faure B, Cruaud C, Samadi S (2013b) The contrasted evolutionary fates of deep-sea chemosynthetic mussels (Bivalvia, Bathymodiolinae). Ecology and Evolution 3: 4748–4766. https://doi.org/10.1002/ece3.749

Turner RD (1973) Wood-boring bivalves, opportunistic species in the deep sea. Science 180: 1377–1379. https://doi.org/10.1126/science.180.4093.1377

van der Heijden K, Petersen JM, Dubilier N, Borowski C (2012) Genetic connectivity between north and south Mid-Atlantic Ridge chemosynthetic bivalves and their symbionts. PLoS One 7: e39994. https://doi.org/10.1371/journal.pone.0039994

Walker JM, Curole JP, Wade DE, Chapman EG, Bogan AE, Watters GT, Hoeh WR (2006) Taxonomic distribution and phylogenetic utility of gender-associated mitochondrial genomes in the Unionoida (Bivalvia). Malacologia 48: 265.

Wang X, Guan H, Qiu J-W, Xu T, Peckmann J, Chen D, Feng D (2022) Macro-ecology of cold seeps in the South China Sea. Geosystems and Geoenvironment 1: 100081. https://doi.org/10.1016/j.geogeo.2022.100081

Weisburg WG, Barns SM, Pelletier DA, Lane DJ (1991) 16S ribosomal DNA amplification for phylogenetic study. Journal of Bacteriology 173: 697–703. https://doi.org/10.1128/jb.173.2.697-703.1991

Won Y-J, Jones WJ, Vrijenhoek RC (2008) Absence of cospeciation between deep-sea mytilids and their thiotrophic endosymbionts. Journal of Shellfish Research 27: 129–138. https://doi.org/10.2983/0730-8000(2008)27[129:AOCBDM]2.0.CO;2

WoRMS (2024) WoRMS taxon details: *Idas* Jeffreys, 1876.

Xu T, Feng D, Tao J, Qiu J-W (2019) A new species of deep-sea mussel (Bivalvia: Mytilidae: *Gigantidas*) from the South China Sea: morphology, phylogenetic position, and gill-associated microbes. Deep

Sea Research Part I: Oceanographic Research Papers 146: 79–90. https://doi.org/10.1016/j.dsr.2019.03.001

Zhang D, Gao F, Jakovlić I, Zou H, Zhang J, Li WX, Wang GT (2020) PhyloSuite: An integrated and scalable desktop platform for streamlined molecular sequence data management and evolutionary phylogenetics studies. Molecular Ecology Resources 20: 348–355. https://doi.org/10.1111/1755-0998.13096

Zhao B, Gao S, Zhao M, Lv H, Song J, Wang H, Zeng Q, Liu J (2022) Mitochondrial genomic analyses provide new insights into the "missing" atp8 and adaptive evolution of Mytilidae. BMC Genomics 23: 738. https://doi.org/10.1186/s12864-022-08940-8

Supplementary material 1

Wood substrate from which *Idas* specimens were collected in this study (Sample ID: TIO2023-1816)

Authors: Qiong Wu, Yi-Tao Lin, Jian-Wen Qiu, Mei Yu Xu, Bing Peng Xing
Data type: jpg
Copyright notice: This dataset is made available under the Open Database License (http://opendatacommons.org/licenses/odbl/1.0/). The Open Database License (ODbL) is a license agreement intended to allow users to freely share, modify, and use this Dataset while maintaining this same freedom for others, provided that the original source and author(s) are credited.
Link: https://doi.org/10.3897/zse.101.142007.suppl1

Supplementary material 2

BI phylogenetic tree of the subfamily Bathymodiolinae based on cox1 and 16S genes

Authors: Qiong Wu, Yi-Tao Lin, Jian-Wen Qiu, Mei Yu Xu, Bing Peng Xing
Data type: png
Explanation note: Numbers represent bootstrap values (only those >0.75 are shown).
Copyright notice: This dataset is made available under the Open Database License (http://opendatacommons.org/licenses/odbl/1.0/). The Open Database License (ODbL) is a license agreement intended to allow users to freely share, modify, and use this Dataset while maintaining this same freedom for others, provided that the original source and author(s) are credited.
Link: https://doi.org/10.3897/zse.101.142007.suppl2

Supplementary material 3

The complete mt genome of *Idas sinensis* sp. nov. (Sample ID: TIO2023-1816B6) and *Idas pacificus* sp. nov. (Sample ID:TIO2023-1816B13)

Authors: Qiong Wu, Yi-Tao Lin, Jian-Wen Qiu, Mei Yu Xu, Bing Peng Xing
Data type: png
Copyright notice: This dataset is made available under the Open Database License (http://opendatacommons.org/licenses/odbl/1.0/). The Open Database License (ODbL) is a license agreement intended to allow users to freely share, modify, and use this Dataset while maintaining this same freedom for others, provided that the original source and author(s) are credited.
Link: https://doi.org/10.3897/zse.101.142007.suppl3

Supplementary material 4

GenBank sequences used for phylogenetic tree construction

Authors: Qiong Wu, Yi-Tao Lin, Jian-Wen Qiu, Mei Yu Xu, Bing Peng Xing
Data type: xlsx
Copyright notice: This dataset is made available under the Open Database License (http://opendatacommons.org/licenses/odbl/1.0/). The Open Database License (ODbL) is a license agreement intended to allow users to freely share, modify, and use this Dataset while maintaining this same freedom for others, provided that the original source and author(s) are credited.
Link: https://doi.org/10.3897/zse.101.142007.suppl4

Supplementary material 5

List of animal species associated with wood substrate and their GenBank accession numbers (Excluding *Idas* spp.)

Authors: Qiong Wu, Yi-Tao Lin, Jian-Wen Qiu, Mei Yu Xu, Bing Peng Xing
Data type: xlsx
Copyright notice: This dataset is made available under the Open Database License (http://opendatacommons.org/licenses/odbl/1.0/). The Open Database License (ODbL) is a license agreement intended to allow users to freely share, modify, and use this Dataset while maintaining this same freedom for others, provided that the original source and author(s) are credited.
Link: https://doi.org/10.3897/zse.101.142007.suppl5

Supplementary material 6

List of genbank accession numbers, biosample accession numbers, and sequence read archive (SRA) data obtained in this study

Authors: Qiong Wu, Yi-Tao Lin, Jian-Wen Qiu, Mei Yu Xu, Bing Peng Xing
Data type: xlsx
Copyright notice: This dataset is made available under the Open Database License (http://opendatacommons.org/licenses/odbl/1.0/). The Open Database License (ODbL) is a license agreement intended to allow users to freely share, modify, and use this Dataset while maintaining this same freedom for others, provided that the original source and author(s) are credited.
Link: https://doi.org/10.3897/zse.101.142007.suppl6

Supplementary material 7

The Best-Fit Models According to AIC

Authors: Qiong Wu, Yi-Tao Lin, Jian-Wen Qiu, Mei Yu Xu, Bing Peng Xing
Data type: xlsx
Copyright notice: This dataset is made available under the Open Database License (http://opendatacommons.org/licenses/odbl/1.0/). The Open Database License (ODbL) is a license agreement intended to allow users to freely share, modify, and use this Dataset while maintaining this same freedom for others, provided that the original source and author(s) are credited.
Link: https://doi.org/10.3897/zse.101.142007.suppl7

Supplementary material 8

K2P distances of cox1 genes in *Idas* species

Authors: Qiong Wu, Yi-Tao Lin, Jian-Wen Qiu, Mei Yu Xu, Bing Peng Xing
Data type: xlsx
Copyright notice: This dataset is made available under the Open Database License (http://opendatacommons.org/licenses/odbl/1.0/). The Open Database License (ODbL) is a license agreement intended to allow users to freely share, modify, and use this Dataset while maintaining this same freedom for others, provided that the original source and author(s) are credited.
Link: https://doi.org/10.3897/zse.101.142007.suppl8